WORLD CONFERENCE ON TIMBER ENGINEERING 2025
BRISBANE, AUSTRALIA

Advancing Timber for the Future Built Environment

CONSIDERATION OF FLUID FORCES ACTING ON PARTS OF WOOD HOUSE UNDER FLOOD

Takahiro Tsuchimoto[1], Shigeru Hirano[2], Yuki Takadake[3]

ABSTRACT: Floods are occurring frequently due to climate change, and it has become difficult to protect residential areas with levees alone, so the Japanese government has shifted its policy to River Basin Disaster Resilience and Sustainability by All. It is necessary to ensure the safety of wood houses even in flooded areas, so we subjected to the model of wood house to investigate the structural safety of wooden houses under the fluid forces caused by flood disaster. As a result, it was suggested that if there is an opening of similar size on the side where fluid force acts and on the opposite side, it may be possible to reduce the pressure receiving area on the verification of the sliding. However, it was also found that on the verification of the overturning using the fluid resistance formula, it may not be possible to reduce the pressure-receiving area.

KEYWORDS: Climate change, Fluid force, Flood, Sliding, Overturning

1 – INTRODUCTION

In recent years, the effects of climate change have led to more severe and frequent water disasters around the world, and in Japan, rainfall and the frequency of flooding are expected to increase.

As a result, in addition to improving and reviewing existing flood control plans, a shift in policy has been made to "River Basin Disaster Resilience and Sustainability by All". This new policy takes measures to be implemented with the cooperation of all stakeholders including the national and local government, private enterprises, and residents in any kind of place around basins including not only river areas and floodplains but also catchments, as shown in Figure 1.

The measures in the floodplains include restricting land use and preventing buildings from flooding in order to secure the human lives and to minimize the damage. However, the mechanical properties or the resilience of wood houses under flood had never grasped.

Therefore, in this paper, hydraulic experiments using a flood flow channel and computational fluid analysis were conducted on a scaled-down model of a wooden house in order to accumulate technical knowledge.

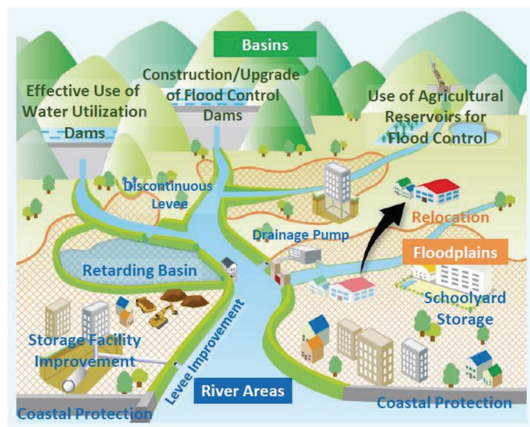

Figure 1. Images of River Basin Disaster Resilience and Sustainability by All.

2 – BACKGROUND

2.1 STRUCTURAL SAFETY UNDER FLOODS

The safe construction methods must be adopted when constructing houses and other buildings within the area where is designated as a flood prevention area.

Specifically, the buildings must be safe against fluid forces (drag and buoyancy) caused by anticipated floods, etc., as

[1] Takahiro Tsuchimoto, Director, Dept. of Building Materials and Components, Building Research Institute, Tsukuba, Japan, tutti@kenken.go.jp

[2] Shigeru Hirano. Manager, Special Construction Planning Department, ICHIJO Co., Ltd., Hamamatsu, Japan, s-hirano@ichijo.co.jp

[3] Yuki Takadate. Senior Research Engineer, Dept. of Structural Engineering, Building Research Institute, Tsukuba, Japan, takadate@kenken.go.jp

https://doi.org/10.52202/080513-0685

stipulated in Notification of the Ministry of Land, Infrastructure, Transport and Tourism No. 1392 of 2021 (hereinafter referred to as the "MLIT Notification"). The fluid forces, F_H caused by anticipated floods, etc. are given by Notification No. 1392 as Equation (1).

$$F_H = \frac{1}{2}\rho C_D B h U^2 \tag{1}$$

where: F_H: Fluid force (kN),
ρ: Density of river water (ton/m^3),
C_D: Drag coefficient (= 2.1),
B: Width of the area where floods act (m),
h: Depth of floods (m),
and U: Flow velocity (m/s)

These are input to the wood house as the horizontal shear force, the lateral load and the rotational moment, and it is necessary to confirm that the wooden house's allowable shear capacity, sliding resistance, and overturning resistance exceed them, respectively.

The horizontal shear force, F_{sh} acting on the 1st story of wood house can be calculated by Equation (2). It is necessary to confirm that it does not exceed the shear capacity.

$$F_{sh} = \frac{1}{2}\rho C_D U^2 \int_{z'}^{H} B(y)dy \tag{2}$$

where: y: Height coordinate of the building (ground level as origin: m)

$$z' = \begin{cases} H, & (H < z_0) \\ \min\left(H - \frac{(H-z_0)^2}{2(2z_1 - z_0)}, z_1\right), & (H \geq z_0) \end{cases},$$

z_0: Height of foundation (m),
and z_1: 1/2 height of the 2nd floor from the ground level (m),

The lateral load causing sliding, F_{as} can be calculated by Equation (3). It is necessary to confirm that it does not exceed the sliding resistance.

$$F_{as} = \frac{1}{2}\rho C_D U^2 \int_{z_2}^{H} B(y)dy \tag{3}$$

$$\text{where: } z_2 = \begin{cases} 0\ (for\ \text{entire}\ building: m) \\ Height\ of\ Foundation * \ (m) \\ \text{Height of sill} ** \ (\text{m}) \end{cases}$$

*: for the shear on the foundation

**: for the shear on the joint between column and sill

For example, the sliding resistance of the entire building is the product of the building weight and the static friction coefficient. The sliding resistance on the foundation and on the sill are the shear strength of the anchor bolts and the shear strength of the column bottom joints, respectively.

The overturning moment, M_r can be calculated by Equation (4). It is necessary to confirm that it does not exceed the overturning resistance.

$$M_r = \frac{1}{2}\rho C_D U^2 \int_0^H B(y)ydy + F_{bu}x_F \tag{4}$$

where: F_{bu}: Buoyant force (kN)
and x_F: Distance between the center of buoyancy and the support point of overturning

The resistance of overturning is the product of the building weight and the horizontal distance between the center of the building weight and the support point of overturning.

2.2 ANALYSIS OF FLOOD DAMAGE TO WOOD HOUSES

The flood damage to wood houses were investigated [1]. The floods surveyed were the floodings of the Kuma River in Kumamoto Prefecture caused by the heavy rains of July 2020, the Chikuma River in Nagano Pref. caused by Typhoon No. 19 of 2019, and the Suemasa River in Okayama Pref. caused by the heavy rains of July 2018.

At first, movies were found on video sharing website that revealed the flow velocity. Movies taken by residents in the damaged areas were also provided. Second, the water depths were clarified by reading them with reference to Google Earth and Google Street View at the site where the movie was taken, as shown in Figure 2, or by investigating and reading the flood marks at the site where the movie was taken. As a result, the several pairs of the flow velocity and the water depth were obtained.

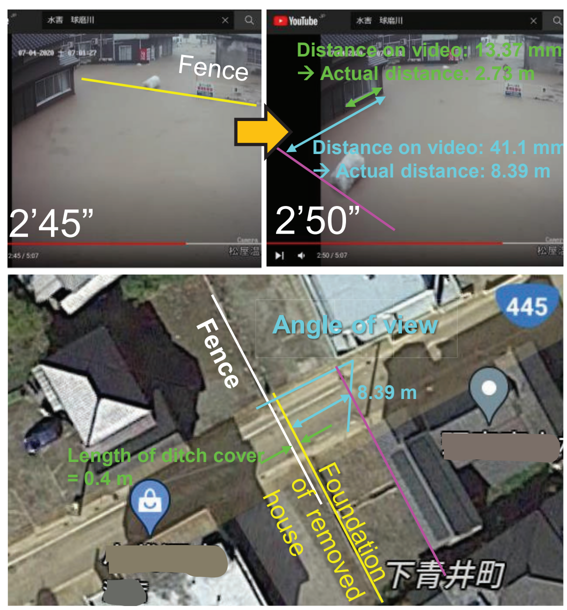

Figure 2. Example of how to estimate flow velocity by reading video and referring to Google Earth and Google Street View.

The water depth and flow velocity that are estimated to have acted on the points where the wooden houses whose damage and structural information was collected were located were distributed at water depths of 0.1 to 5 m and flow velocities of 0.1 to 8 m/s.

The obtained water depth and flow velocity were substituted into equations (2) to (4) to calculate the horizontal shear force, lateral load, and overturning moment acting the house, respectively. The shear capacity

https://doi.org/10.52202/080513-0685

of each house was compared with the horizontal shear force acting on it, and their verification ratios were calculated and shown in Figure 3. Then, the sliding resistance of each house was compared with the lateral load causing sliding acting on it, and their verification ratios were calculated and shown in Figure 4. The negative ratio indicates that the buoyancy is more than the weight of the house.

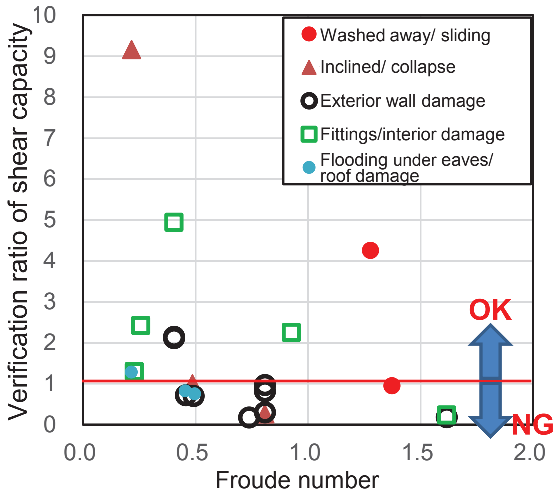

Figure 3. Comparison of verification ratio (shear capacity of house/ horizontal shear force acting on it) with Froude number.

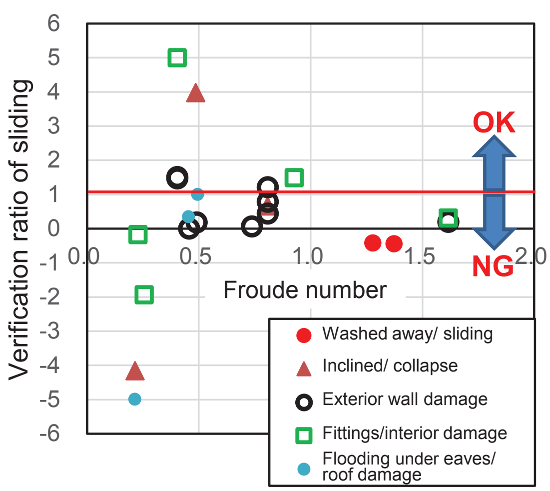

Figure 4. Comparison of verification ratio (sliding resistance of house/ lateral load acting on it) with Froude number.

As a result, it was clarified that the theoretically estimated damage state often does not correspond to the actual damage state. In other words, it is possible that many wooden houses that would have suffered shear failure or sliding avoided the collapse or the sliding due to damage to the exterior walls, as shown in Figure 5 as examples. We therefore came up with the idea that the scaled-down model of wood house with and without openings were subjected to the hydraulic tests using the flood flow channel and the numerical fluid analysis.

Figure 5. Examples of wood houses that may have avoided the collapse or the sliding due to damage to the exterior walls/ components.

3 – SPECIMEN AND TEST CONDITION

3.1 SCALED SPECIMEN

The specimen with 1,212 mm square was made as 1/3 scaled model of the actual light frame construction house, as shown in Figure 6. However, the studs and sheathing panels were made of 204-dimension lumber and 12 mm thick structural plywood, respectively, to prevent deformation due to fluid forces. The removable openings were installed in the center of each perimeter of the specimen, which could be removed according to the test conditions, as shown in Table 1 [2].

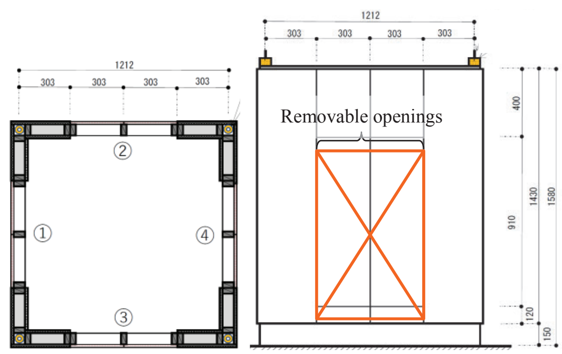

Figure 6. Schematic plan (left) and elevation of 1/3-scale specimen.

Table 1. Specifications of tested specimen.

Case of specimen	Length of one side (mm)	Length of opening (mm)			
		①	②	③	④
1	1,212	0	0	0	0
2	1,212	606	0	0	0
3	1,212	606	606	0	0
4	1,212	606	606	606	0
5	1,212	606	0	0	606
6	1,212	606	606	0	606
7	1,212	606	606	606	606

3.2 TESTING METHODS

The hydraulic tests were conducted using the tsunami/ flood channel (Figure 7) of the Central Research Institute of Electric Power Industry, Japan. The test channel section is 20 m long, 4 m wide and 2.5 m deep with a maximum water storage capacity of 650 t. The operating method of the flow channel control system was adjusted so that the

https://doi.org/10.52202/080513-0685

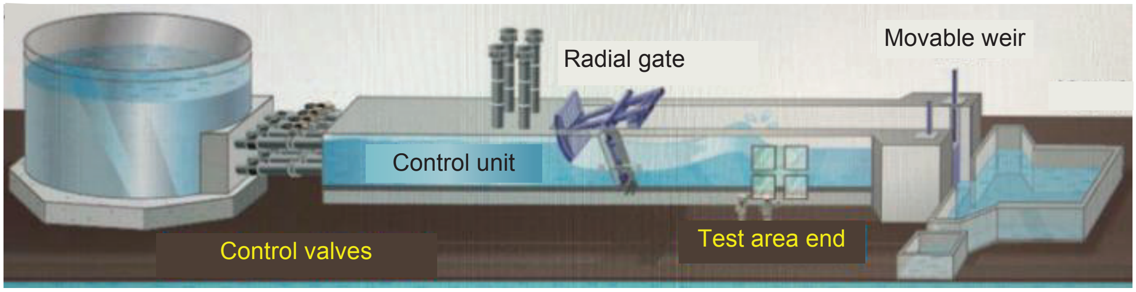

Figure 7. The tsunami/flood channel applied for the hydraulics test.

water flow near the center of the test channel reached the target water depth and flow speed shown in Table 2 when no test specimen was installed, and was used as the input wave.

Table 2. Applied water flow conditions.

Water flow	Water depth (m)	Flow velocity (m/s)	Initial water depth (m)	Froude number (*Fr*, *ref.*)
a	0.45	2.0	0	0.95
b	0.65	1.0	0.25	0.40
c	0.65	2.0	0.15	0.79
d	0.65	4.0	0	1.58
e	0.85	2.0	0.25	0.69

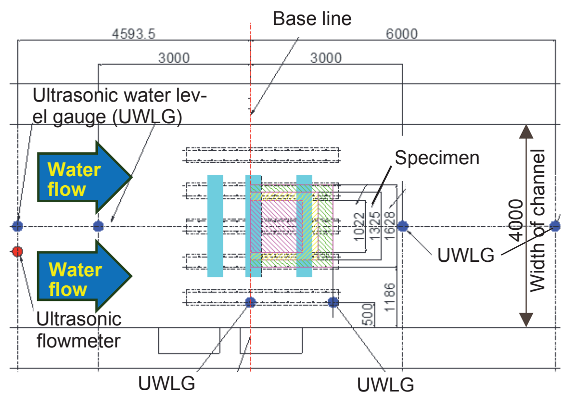

Figure 8. Location of specimen and sensors.

3.3 MEASURING METHODS

A slider plate with a friction coefficient of about 0.06 was set at the bottom of the tsunami/flood flow channel, and the specimen was installed above it. The water depth and flow speed were measured by the ultrasonic water level gauge (UWLG) and the ultrasonic flowmeter, respectively, at each location shown in Figure 8. As shown in Figure 9, the tie rods were embedded in the corners of the specimen, and the load cells installed above and below the tie rods measured the loads when the vertical upward and downward forces were applied, respectively. A wire extending to the upper part of the channel via a pulley was connected the lowest part of the specimen, and the horizontal force was measured using a load cell installed at the end of the wire. Wave pressure gauges were installed at 6 locations at 0.20, 0.35, 0.50, 0.65, 0.85, and 1.20 m from the bottom of the frame in front of the specimen to measure wave pressure due to water flow.

In addition, for some test cases, the water flow was applied twice, and after confirming the reproducibility of the water flow and the stability of the specimen once, the water flow was input one more time. The average value (noise canceled) of each measurement value in the quasi-steady flow section was calculated, and this was used as the wave pressure and load in each part.

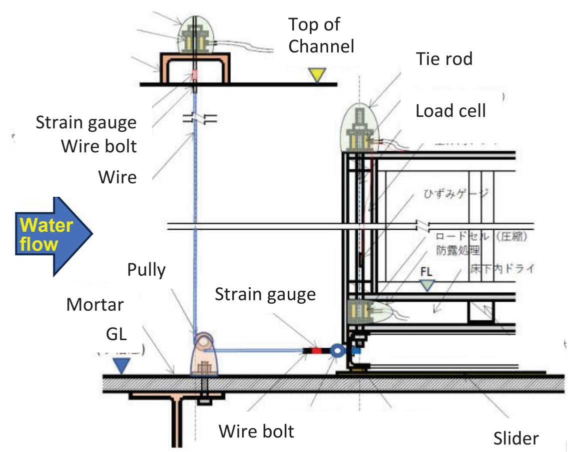

Figure 9. Cross section of specimen and layout of sensors.

4 – RESULTS OF HYDRAULIC TESTS

4.1 HORISONTAL FORCE CAUSING SLIDING

The wave force was obtained by multiplying the wave pressure gauge measurement by the pressure-receiving area. It was defined that the wave (fluid) force was input by the water flow to the scaled specimen and the lateral force acted on it. The relationships between the horizontal force (wave force, F_H) calculated from the measured value of the wave pressure meter and the measured value of the load cell installed at the tip of the wire (horizontal force,

P) for the cases 1 to 7 are shown in Figure 10. The horizontal force acting on the specimen was about half of or less than the wave force even without opening. However, in the cases 2 to 4, horizontal force were over the half of the wave force and larger than that in the case 1 without an opening.

And, the ratio of the horizontal force in each case to the horizontal force in the case 1 is shown in Figure 11. In the cases 2 to 4, it can be seen that the horizontal forces is over the horizontal force in the case 1 without openings, especially when the water depths are relatively large and the flow velocities are high in the water flows c to e. On the other hand, in the case 5 to 7, it was clarified that the horizontal force acting the scaled specimen were less than or equal to that of the case 1 withoout openings, regardless of any water depths and any flow velocities.

Since the opening area ratio is 0.5, it was suggested that if there is an opening on the front side and a similar opening on the downstream side, it is possible to reduce the pressure receiving area in the sliding verification.

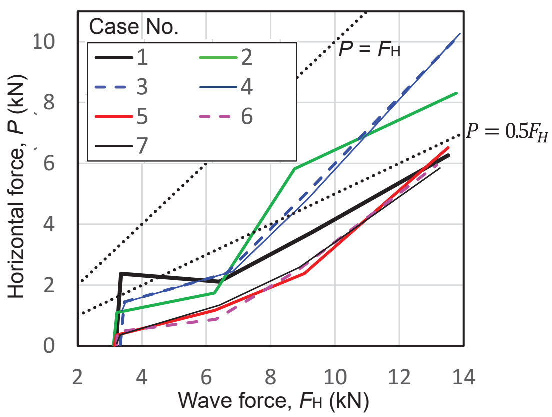

Figure 10. Relationships between wave force and horizontal force.

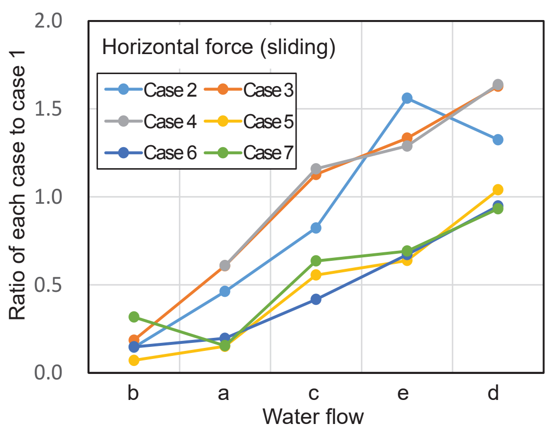

Figure 11. Ratio of horizontal force of each case to case 1.

4.2 OVERTURNING

The wave force moment (M_r) was calculated by multiplying the wave force by the height where the wave pressure gauge installed. The overturning moment (M_B), which takes into account the weight of the inflowing water, is calculated from the load cell measurements and compared with the wave force moment, as shown in Figure 12.

The overturning moment acting the scaled model was about half of the wave force moment, except for the case 3. There is a possibility that not all of the moment of wave force acts as the overturning moment of the scaled model. The wave force moment and overturning moment of the case 2 with opening only on the entrance side are almost the same as those of the case 1, but it can be seen that an extremely large overturning moment acts on the case 3 with asymmetric opening layout. The cases 6 and 7 are the same as the case 5 with an additional opening, but are subjected to the overturning moment that is often larger than that of the case 5.

And, the ratio of the overturning moment in each case to that of the case 1 was calculated and shown in Figure 11. Under the condition with small water depth and slow water velocity, the overturning moment was extremely large. Even under the condition with large water depth and rapid water velocity, the ratio were about the same or more than 1.0.It was suggested that it is not possible to reduce the pressure receiving area in the overturning verification.

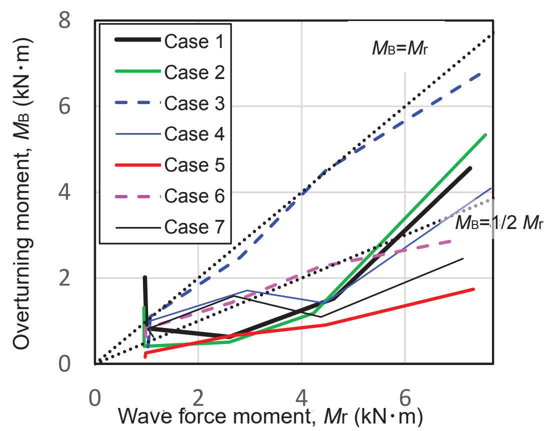

Figure 12. Relationships between wave force and overturning moment.

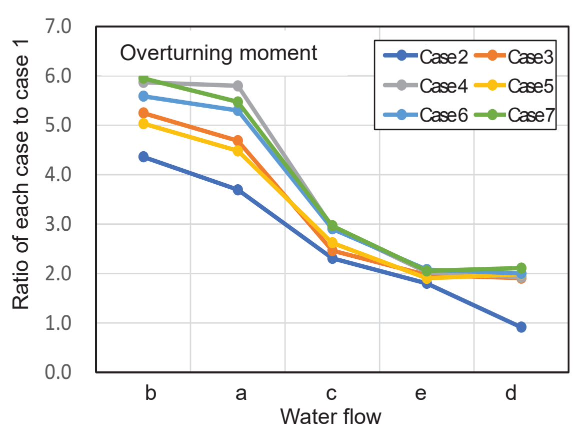

Figure 13. Ratio of overturning moment of each case to case 1.

https://doi.org/10.52202/080513-0685

5 – COMPUTATIONAL FLUID ANALYSIS

5.1 ANALYSIS CONDITION

An analytical model was constructed that accurately reflected the detailed dimensions of each part of the test specimen shown in Figure 6 and Table 1. The analytical model was placed at the center of 4 m wide channel, as in the hydraulic test, which corresponds to the channel blockage rate of 30 %.

For the computational fluid analysis, gas-liquid two-layer flow analysis was used with OpenFOAM. The turbulence model was the standard Smagroinsky model (model constant Cs = 0.13) of Large Eddy Simulation (LES). The model mesh was based on 100 mm, and the mesh near the model was segmented in five stages to 3.125 mm using snappyHexMesh.

The Navier-Stokes equations were developed over time using a first-order accuracy implicit method (Euler method). They were discretized using second-order accuracy upwind finite difference. Each side and top surface of the analysis domain were under slip conditions, and the floor and wall surfaces of the model were under no-slip conditions. The inflow boundary was under a no-gradient condition.

An automatic time step was used so that the Courant number did not exceed 0.9. In the analysis, the calculation was started with the initial water depth set to the same height as the initial target water depth, and each statistical value was evaluated using data for 10 seconds after the horizontal force acting on the model reached a quasi-steady state.

In addition to the above, the analyses were conducted in which the channel width was changed from the initial 4 m to 8 m and 16 m, corresponding to blockage rates of 15% and 7.5%, respectively. It was found that there was almost no interference of reflected waves from the side walls under the condition of the 16 m wide channel, so the other analyses were also conducted when the channel width was set to 16 m.

5.2 COMPARISON WITH TESTS RESULTS

5.2.1 Horizontal force that causes sliding

The relationship between wave force and horizontal force obtained from the fluid analysis is shown in Figure 14 under the condition of 4 m wide channel and in Figure 15 under the condition of 16 m wide channel. In the hydraulic tests, the horizontal force causing sliding was generally smaller than the wave force (Figure 10), but in the fluid analysis, the wave force and horizontal force showed almost the same values regardless of the presence or absence of the influence of the side walls.

The ratio of horizontal forces in each case to that in Case 1 obtained by fluid analysis was shown in Figure 16 under the condition of 4 m wide channel and in Figure 17 under the condition of 16 m. In the hydraulic tests (Figure 11) under high Froude number input conditions, it is significant clear that the cases with openings only on the entrance surface or on the surface perpendicular to it, the larger horizontal force acts than the case without openings.

On the other hand, when there is an opening on the downstream side opposite to the entrance surface, the horizontal force in hydraulic experiments, is smaller than the case without openings, except for the case of the supercritical water flow d. In the fluid analysis, in the case with opening only on the entrance surface and the opposite side of it, the horizontal force is reduced to about 0.6 under the side wall effect and about 0.8 under no side wall effect. However, it can be seen that the reduction of the horizontal force is mitigated when there are openings not only on the entorance surface and the opposite side but also on the side perpendicular to it.

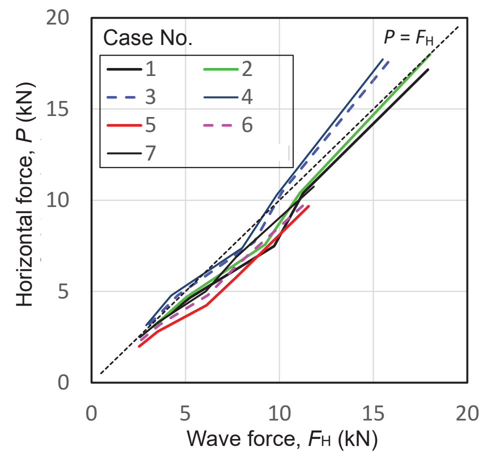

Figure 14. Relationships between wave force and horizontal force obtained from fluid analysis under 4 m wide channel.

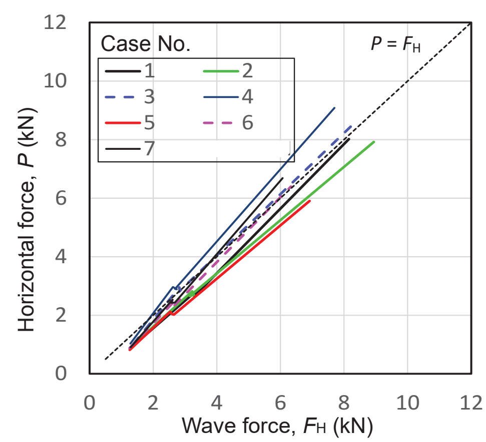

Figure 15. Relationships between wave force and horizontal force obtained from fluid analysis under 16 m wide channel.

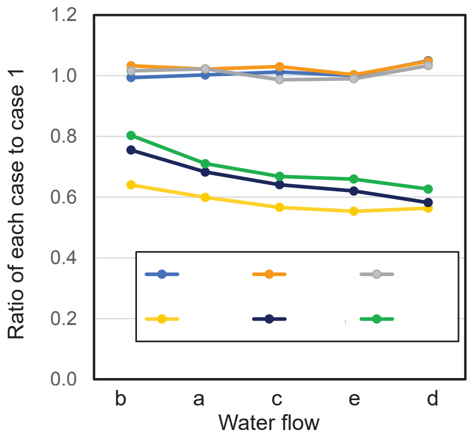

Figure 16. Ratio of horizontal force of each case to case 1 obtained from fluid analysis under 4 m wide channel.

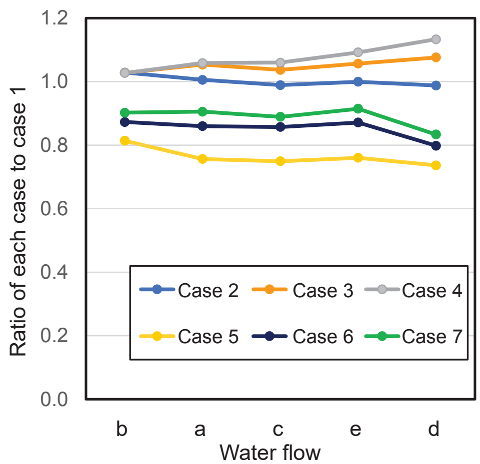

Figure 17. Ratio of horizontal force of each case to case 1 obtained from fluid analysis under 16 m wide channel.

5.2.2 Overturning moment due to wate flow

The relationship between the wave force moment, *M*r and the overturning moment acting the analyzed specimen obtained in the fluid analysis were shown in Figure 18 under the condition of the 4 m wide channel and in Figure 19 under the condition of the 16 m wide channel. In the hydraulic tests (Figure 12), the overturning moment acting the scaled model was about half of the moment calculated from wave pressure, except for the case 3. However, in the fluid analysis, the value of both moments were almost the same regardless of the presence or absence of the influence of the side wall..

And, in the hydraulic tests, the overturning moment of the cases 2 to 4 with opening on the entrance face and without opening on the opposite side of the entrance face often have larger overturning moment than case 1 without opening, but these is not necessarily the case in the fluid analysis. Then, in the hydraulic tests, the overturning moment of the cases 5 to 7 with opening on the opposite side of the entrance face may be larger or smaller than case 1 depending on the strength of the water flow. On the other hand, in the fluid analysis, those of the case 5 to 7 were often larger than case 1 under the influence of the side wall, but those of the case 5 were perfectly the same as the case, and those of the case 6 and 7 were clearly larger than the case 1 and 5.

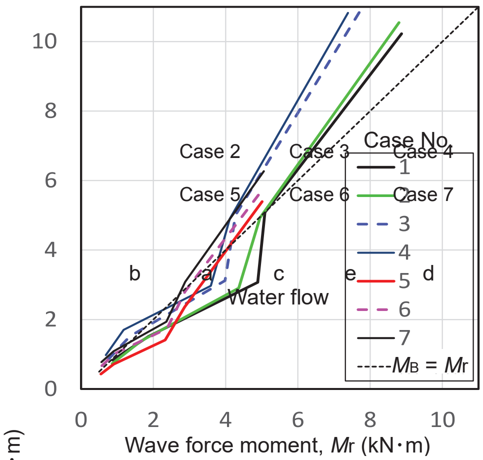

Figure 18. Ratio of wave force moment and overturning moment obtained from fluid analysis under 4 m wide channel.

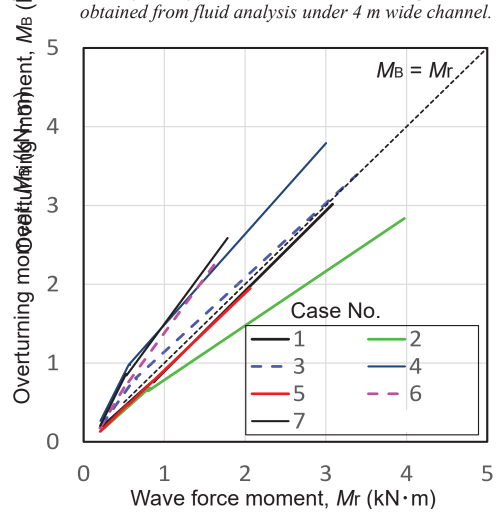

Figure 19. Ratio of wave force moment and overturning moment obtained from fluid analysis under 16 m wide channel.

6 – CONCLUSION

In order to study the possibility of applying a reduction factor for the pressure-receiving area of house with openings, the hydraulics test using the scaled-down models of wood houses with and without openings were conducted. And, the conputational fluid analyses about the hydraulics tests were conducted.

The results can be summarized as follows:

If there is opening of similar size on the side where fluid force acts and on the downstream side, it may be possible to reduce the pressure receiving area on verification of the sliding.

https://doi.org/10.52202/080513-0685

Even if there are openings of similar size on the side where fluid force acts and on the downstream side, it may not be possible to reduce the overturning moment. Because, it didn't decrease under that condition of opening.

Even if there are openings on the side of the fluid force acting, in the case without opening on the downstream side, the horizontal force and overturning moment can not only be not reduced, but often may increase actually also.

7 – REFERENCES

[1] T. Tsuchimoto, Y. Yamazaki, S. Higuchi, T. Inoue, N. Imai, S. Matsudome, Y. Oshima, S. Masuda, K. Shibanuma and J. Sakuma: “Studies on the fluid force acting on wood houses under the flood Part 1-5”. Summaries of technical papers of annual meeting, Architectural Institute of Japan, C–1 (Structure III), (2022), pp. 569–578.

[2] J. Sakuma, K. Shibanuma, S. Hirano, and T. Tsuchimoto: “Verification of Fluid Force by Hydraulic Tests on Wood House Model Part 1–3”, Summaries of technical papers of annual meeting, Architectural Institute of Japan (2023), Z–1, pp. 245–250.

ACKNOWLEDGEMENT

This research project was carried out as a part of theme “Development of flood prevention technology for wood houses to reduce damage under the basin flood control” funded by the Cabinet Office's Public/Private R&D Investment Strategic Expansion Program (PRISM) in the infrastructure disaster prevention area. I’d like to thank Dr. Naoto Kihara, Research Promotion Manager, Meteorological and Fluid Science Research Division, Sustainable Systems Research Headquarters, Central Research Institute of Electric Power Industry, for his valuable advice. I’d like to thank Junzo Sakuma, President of Design Studio Sakuma, for their assistance in designing the scaled specimen.